International Journal of Precision Engineering and Manufacturing
https://doi.org/10.1007/s12541-021-00479-0

Online ISSN 2005-4602
Print ISSN 2234-7593

REGULAR PAPER

Additively Manufactured Custom Soft Gripper with Embedded Soft Force Sensors for an Industrial Robot

Savas Dilibal[1,2] · Haydar Sahin[1] · Josiah Owusu Danquah[3] · Md Omar Faruk Emon[2] · Jae-Won Choi[2]

Received: 7 December 2020 / Revised: 11 January 2021 / Accepted: 24 January 2021

Abstract

Soft robotic grippers are required for power grasping of objects without inducing damage. Additive manufacturing can be used to produce custom-made grippers for industrial robots, in which soft joints and links are additively manufactured. In this study, a monoblock soft robotic gripper having three geometrically gradient fingers with soft sensors was designed and additively manufactured for the power grasping of spherical objects. The monoblock structure design reduces the number of components to be assembled for the soft gripper, and the gripper is designed with a single cavity to enable bending by the application of pneumatic pressure, which is required for the desired actuation. Finite element analysis (FEA) using a hyperelastic material model was performed to simulate the actuation. A material extrusion process using a thermoplastic polyurethane (TPU) was used to manufacture the designed gripper. Soft sensors were produced by a screen printing process that uses a flexible material and ionic liquids. The grasping capability of the manufactured gripper was experimentally evaluated by changing the pneumatic pressure (0–0.7 MPa) of the cavity. Experimental results show that the proposed monoblock gripper with integrated soft sensors successfully performed real-time grasp detection for power grasping.

Keywords Material extrusion · Screen printing · Soft robotics gripper · Soft force sensor · Power grasping

1 Introduction

Soft robotic grippers installed on robotic manipulators are widely used in electropneumatic systems for applications in handling and packaging [1–3]. Additive manufacturing technology has been used to fabricate soft robotic grippers using hyperelastic materials such as thermoplastic elastomer (TPE). The integration of additive manufacturing with advanced design technology enables the production of soft robotic gripper mechanisms that are increasingly employed in industrial robots [4, 5].

The geometric or material-based asymmetry of pneumatically actuated soft robotic grippers causes radial expansion, axial contraction and/or bending of the gripper with the injection of pressurized air. Material-based asymmetry is used in additive manufacturing via multi-material printing for tuning of material properties and the fabrication of on-demand application-specific soft gripper in soft robotic applications [6–8]. In particular, injecting compressed air into a cavity inside a soft gripper enables a bending motion, resulting in controllable actuation [4]. The bending motion of a soft robotic gripper is mainly dictated by the geometry of the cavity and its internal air pressure [9]. Moreover, the design criteria for the gripper geometry depends on the type of grasping required, such as power grasping or precision grasping [10]; thus, application-specific designs of soft grippers can provide custom-made grasping solutions for industrial robots [11, 12]. Here, power grasp is referred to as a robotic grasp type with a maximum contact surface area between the gripper and object enabled by stabilized force without slipping [13]. In particular, to grasp a spherical object, a bending motion is required that changes the shape of the gripper so that it can conform to and grasp the object. The cavity geometry and the inner pressure of the cavity are the application-dependent constraints that determine the

✉ Savas Dilibal
savas.dilibal@gedik.edu.tr

✉ Jae-Won Choi
jchoi1@uakron.edu

1 Mechatronics Engineering Department, Istanbul Gedik University, 34987 Istanbul, Turkey

2 Mechanical Engineering Department, The University of Akron, Akron, OH 44325, USA

3 Civil and Environmental Engineering Department, Cleveland State University, Cleveland, OH 44115, USA

Published online: 10 February 2021

radius of curvature for the soft gripper. Moreover, Euler–Bernoulli equation for beam theory can be used to formulate the radius of curvature in terms of the internal moment, the modulus of elasticity, and inertia [14, 15]. In addition to the numerical solution, the results from experiments and finite element analysis (FEA) can be used to evaluate the grasping capability for the finalized design for a prototype soft gripper.

It has been shown that motion control of the soft robotic grippers can be enhanced through the addition of integrated sensors. Research has been conducted to develop integrated soft sensing and actuation systems [16, 18]. Compared to general-purpose commercial sensors, custom-made soft force sensors can offer higher sensitivity that enables more accurate measurement of the grasping force to be obtained [19, 20]. Soft force sensors have been employed for numerous applications such as robotics [17], prosthetics [18], and wearable electronics [19].

Recently, the authors have reported the incorporation of ionic liquid (IL) into a stretchable polymer to fabricate a solid-state pressure sensor [20]. Viscoelastic polymers having ILs provide ionic conductivity and electrochemical stability, which makes them suitable for use as soft sensors in soft robotic actuators. In applications such as robotics or prosthetics, there are moveable parts that are subjected to bending and flexing. Therefore, sensors for these applications need to be flexible and stretchable. ILs with a stretchable polymer can create a pressure-sensitive soft and stretchable membrane. IL-based polymeric force sensors demonstrate superior performance compared to commercial sensors in terms of stretchability, reliability, and consistency [20]. In addition to electrochemical stability, IL provides the freedom to configure and design the sensor according to the custom-made application. The sensitivity of the sensor can be adjusted by varying the IL concentration and IL/polymer membrane geometry. Thus, ILs in soft pressure sensors provide more controllability on sensor performance along with better efficiency. Moreover, the development of 3D printable inks with ILs can offer the opportunity to build the integrated gripper with pressure sensors in a single manufacturing system.

In this study, a gripper with integrated soft force sensors was additively manufactured using a material extrusion process and screen printing. Numerical analysis and FEA were used to design the gripper. Additionally, the experiments were conducted to demonstrate the capabilities of the gripper for the power grasping of spherical objects.

2 Design, Materials and Methods

2.1 Design of Soft Robotic Gripper

To successfully achieve the power grasping of spherical objects, the design for the soft robotic gripper proposed in this study has a monoblock structure, which reduces the complexity of the gripper design such that it has no additional components and does not require any assembly. The proposed gripper incorporates three fingers; detailed drawings of one soft finger are shown in Fig. 1, which shows a geometrically gradient design for the segments of the finger where a taper angle of 8.3° was implemented to induce the bending motion of the fingers [22]. This taper angle is selected from the previous work of the authors [22]. Once air pressure is applied to the cavity of each segment, the cavity will inflate; because the base portion of the segment (i.e., the lower part) is fixed and the upper part of the segment is free, inflation of the cavity will induce a bending motion in the segment. As some dimensions of the cross-sections of the finger segments (such as B_i, $h_{i,}$ and H_i) vary according to the gradient geometry of each section, while other dimensions (such as b, w, d, t, $R_{in,}$ and R_{out}) remain constant (as shown in Fig. 1d, e), the cavity in each section will have a unique volume upon inflation; thus, each segment of the finger will have a different bending angle. The overall bending angle for the finger is the combined effect of the angles generated for each segment. The bending angles for the fingers were analytically and experimentally investigated, as discussed in the following section.

2.2 Additive Manufacturing of the Soft Robotic Gripper

A material extrusion process using a commercially available 3D printer (a model CR-10S printer from Creality3D, Shenzen, China) was utilized to fabricate the soft robotic grippers. A commercially available TPU filament having a diameter of 1.75 mm and a Shore A hardness of 85A was provided by the Shenzhen Esun Industrial Company (Shenzhen, China). The grippers were fabricated using the following print parameters: a nozzle diameter of 0.4 mm, an extruder temperature of 232 °C, and a layer thickness of 0.1 mm. The print orientation was selected for the inner surfaces of the fingers to be in contact with the print-bed, resulting in no need for support structures. The layer width which is used during slicing the object for additive manufacturing is 100%. The lower thickness values than 1.5 mm cause the leakage on the walls of the fingers when the pressurized air is applied. Many trials have been made to determine the minimum thickness level (1.5 mm) without air leakage.

2.3 Flexible Tactile Sensors

The proposed soft force sensor, which is presented in Fig. 2, has five layers: top and bottom insulation layers (shown in yellow in Fig. 2a, b), two conductive electrodes that overlap one another (shown in black), and a pressure-sensitive layer between the conductive electrodes (shown in red in

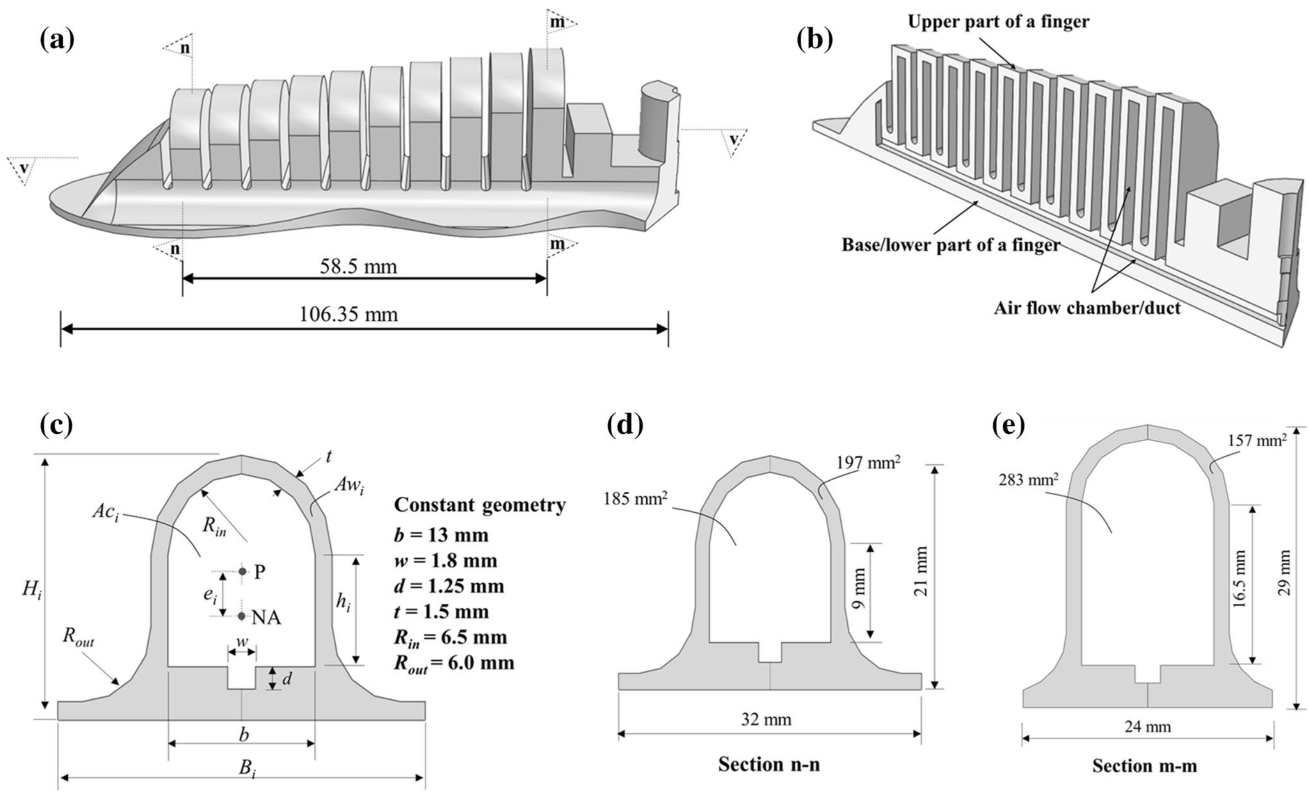

Fig. 1 3D model and schematic diagrams for a finger of the proposed soft gripper: **a** 3D model of a soft finger and **b** a cross-sectional view of the finger showing details of the air flow chamber. **c** Typical cross section for a finger segment (where b, w, d, t, Rin and Rout are constants with the values indicated and where Bi, hi, Hi, Aci, and Awi vary along the longitudinal direction). Exact dimensions in cross sections of two segments: **d** segment n–n and **e** segment m-m

Fig. 2b)-all of which are stretchable [20]. The insulation layers were manufactured using the commercial photopolymer TangoPlus FLX930 (manufactured by Stratasys, Eden Prairie, MN), which produces a stretchable film once it has been polymerized using ultra-violet (UV) light. To fabricate the conductive electrodes, a multi-walled carbon nanotube (MWCNT)–based composite material was prepared by dispersing 5 wt.% MWCNT into TangoPlus. A pressure-sensitive intermediate layer was fabricated by mixing 2 wt.% IL, 1-ethyl-3-methylimidazolium tetrafluoroborate (EMIMBF4; Sigma-Aldrich) in TangoPlus and subsequently photo-polymerizing the prepolymer blend. The IL/prepolymer blend was prepared by using a DAC 150.1 FVZ-K high-speed mixer (FlackTek, Inc., Landrum, S.C., USA), where the IL and the TangoPlus were mixed at 2500 rpm for two minutes. The five-layer sensor was

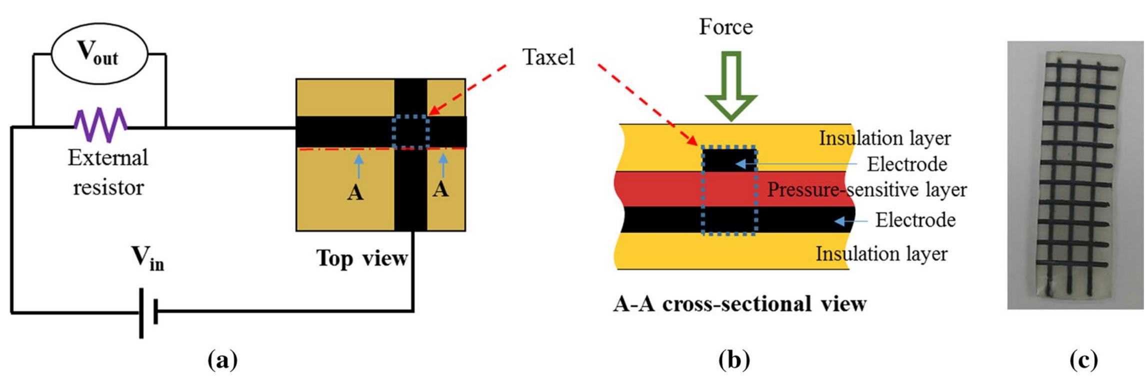

Fig. 2 Schematic diagrams of the sensor architecture showing **a** a top view of the sensor and external circuit and **b** a cross-sectional view (A-A) of the sensor showing the five layers; **c** the printed tactile sensor

fabricated using casting and screen printing; a more detailed discussion of the process used to manufacture the sensor can be found in our prior work [20]. The manufactured tactile sensor was embedded in the 3D printed fingers (Fig. 4).

In the architecture of the soft force sensor shown in Fig. 2, the locations where conductive electrodes cross over one another (the area bounded by a blue dashed line Fig. 2a, b) is the contact pressure–sensing unit that is referred to as a *taxel*. When force is applied to the taxel, the electrical resistance of the soft force sensor will change due to the elastic deformation in the intermediate layer (shown in red in Fig. 2b). An electrical circuit diagram for a soft force sensor with a single taxel is shown in Fig. 2a.

To measure the change in resistance under force, each *taxel* is connected to a potential divider where the voltage output across the external resistor was taken as signal output. When the soft force sensor is connected to an external resistor and an input voltage (V_{in}) is supplied by an external power supply, the output voltage (V_{out}) across the external resistor can be measured to specify the response of the sensor to an applied force. The soft force sensor used in this study (Fig. 2c) was designed with dimensions of 55 mm × 16 mm × 2.5 mm, which is large enough to accommodate the shape of the soft fingers of the proposed gripper. In each soft force sensor, a total of 33 taxels with dimensions of 1 mm × 1 mm × 250 µm were created; three taxels from each sensor were used for the current and future research. The sensitivity (i.e. gauge factor) and dynamic range have been characterized in our prior work [20]. The sensitivity of the sensor was calculated in terms of relative change in resistance per unit strain that varied from 0.9 to 1.5. The sensor used in this work was found to be sensitive in the range of 50 kPa to 1.5 MPa with a dynamic range of 30 dB. Also, the sensor demonstrated reliability for repeated load [20].

2.4 Grasping Experiments

Prior to testing, the soft force sensors were installed on the fingers of the soft robotic gripper, and the total weight of the resulting prototype was 108 g. An experimental setup was designed and implemented for the calibration of the soft force sensors and the measurement of the grasping force of the prototype gripper. The test setup for the sensor calibration (shown in Fig. 3) included an external power supply, an oscilloscope, and a multi-meter for measuring the potential difference under the applied force. The input voltage of 24 V was provided by the external power supply. The number of active taxels to be measured was selected based on the effective area of contact between the finger and the grasped object. In this study, three active taxels were selected in the force sensor that was attached to each finger: one taxel in the proximal area, one taxel in the area of the midpoint, and one taxel in the distal area. The detailed assembly of the taxels to the data acquisition system is shown in Fig. 3. The average voltage of the measured potential differences which were received from the three taxels was used.

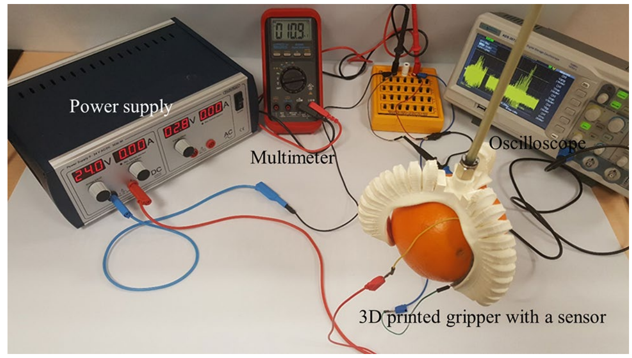

Fig. 3 The experimental setup for the calibration of the soft force sensor of the gripper

The setups used for the experiment and the finite element model for the measurement of the gripping force of the soft robotic gripper are shown in Fig. 4. In the experimental setup, the gripping force of the soft fingers was measured via manipulandum. The manipulandum contains a static load cell with a 10 N measurement range. The calibrated load cell (ESP-10, Transducer Techniques, Temecula, USA) was used to measure the gripping force from the fingers. The soft force sensors were attached in the middle of the inner surface of the fingers using a double-sided adhesive tape (3 M VHB 4910F).

3 Bending Analysis

Bending analysis was conducted using a numerical approach, finite element analysis, and an analysis of the experimental results. The approaches used in each analysis are discussed in greater detail in the sections below.

3.1 Numerical Approach

The bending angle was analyzed by deriving an equation under the different internal pressure inputs. The single soft finger geometry (Fig. 1) used for this bending analysis has variable cross-sections along the entire length, unlike the soft grippers considered in other studies in the literature [14, 15]. Such differences in the geometrical details at the first and last chambers are illustrated in Fig. 1d, e. However, for the analytical derivation, the only dimensional change considered important from segment to segment is the height (h_i). Moreover, since the applied pressure increases at a constant and slow rate, the actuator is assumed to operate under a quasi-static, fixed-free (cantilever beam) boundary condition, in which one end is completely restrained against

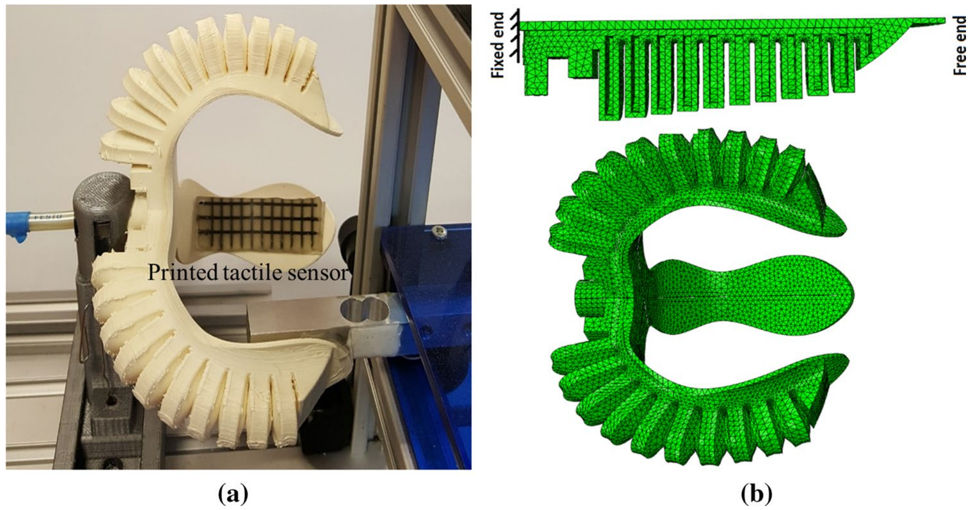

Fig. 4 The experimental and finite element model setup for the measurement of the gripping force of the soft robotic gripper via load cell **a** soft gripper with a tactile sensor **b** the corresponding FEA model

translation and rotation whilst the other end is free to translate and/or rotate. From derivations outlined in the appendix, the relation between the angle of rotation, θ and the applied pressure, P is given as

$$\theta = mP^2 + nP \tag{1}$$

where m and n are constants accounting for the material and geometrical properties of the actuator. Here we used, m = 56 and n = 135 for the TPU material and geometry considered.

3.2 Finite Element Analysis

The Ogden hyperelastic material model was used in the finite element analysis. This model has been used to characterize the response of rubbery materials under biaxial/uniaxial tension and compression in the past [22, 24]. In this study, the model was used first to capture the non-linear stress versus strain behavior of the TPU material, and then utilized for simulating the soft finger contact mechanics [25]. Detailed mathematical backgrounds and applications of the model are provided in the literature [26, 27]. A summary of the equations deemed important for the present task is given in the appendix.

For TPU, the values used in the Ogden model for the moduli μ_k and exponent α_k using $N=3$ are as follows: μ_1 =0.635248209, α_1= 6.97509779, μ_2= 1.219182 × 10^{-6}, α_2= 19.4288377, μ_3 = 10.9205706 and α_3= − 2.61524912, as determined in a study by Dilibal et al. [23].

In this study, the finite element simulation of the soft robotic actuator was conducted using Abaqus/Standard finite element analysis software [28]. The algorithm used in *Abaqus* automatically accounts for the nonlinearity due to the large deformation of the soft material. *Abaqus* also includes a large collection of continuum elements that can be used for the geometry discretization. The continuum solid element C3D10H, which is a 10 node quadratic hybrid tetrahedron, was selected for modeling the finger design; to ensure accuracy while decreasing the computational burden, only half of the symmetrical single finger model was analyzed. Based on the preliminary mesh convergence, a total of 16,359 elements was deemed sufficient for the mesh discretization. In this study, the mesh size ratios were varied successively from 5 to 1. The corresponding output of the effective von Misses stress and maximum displacement at the tip of the soft robotic finger were measured against the computational time after each mesh refinement. Additionally, the boundary conditions required for each symmetric portion of the model as well as those representing the fixed-free conditions were specified. The contact between the grasping portion of the soft robotic finger and the more rigid spherical object was accounted for by using the general surface-to-surface contact model in *Abaqus*. Although the soft deformable body (the finger of the gripper) will initially come into contact with the more rigid spherical object over a small area, the area of contact will increase as the finger conforms to the outside curvature of the spherical object [29].

A quasi-static analysis accounting for both material and geometrical non-linearity was performed using an unconditionally stable, fully-implicit, backward Euler difference integration scheme. In the loading step, the inner walls of the soft gripper were subjected to incrementally increased internal pressure (from 0 to 0.7 MPa) at a slow loading rate of 1×10^{-2} MPa/sec. Notwithstanding the likelihood of anisotropy (common in several AM printed materials), the selected material model and related parameters were based on our earlier experiments and other reported findings in the literature which indicated negligible differences in the TPU material in different directions when tested under very slow rates [33, 34]. In particular, Hohime et al. [33] tested several AM TPU samples in the axial, transverse, and 45 degree angles under different temperatures to study the effect of the AM parameters on the stress–strain responses. Their study showed that over a significant strain magnitude, the stress–strain responses were similar in all directions, indicating that it is possible to produce isotropic mechanical properties in printed TPU samples.

The bending deformation under pressurized air was examined during the loading step using numerical simulation. The maximum bending deformation of the fingers was obtained in a contact-free bending condition, and the measured maximum gripping force was obtained when the fingers were grasping a spherical object.

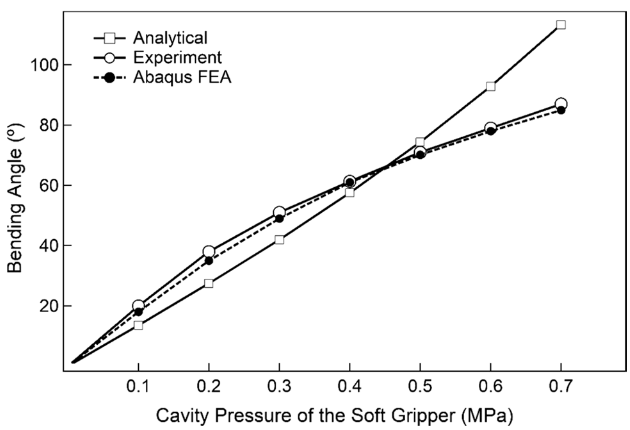

Fig. 5 The increase of the bending angle of a single soft finger with cavity pressure for the experimental, numerical (analytical) and finite element model results

4 Results

4.1 Bending Experiments and Simulation Results

The changes in the bending angle with the cavity pressure from the experimental, numerical, and finite element simulation results are shown in Fig. 5. From this figure, it can be noticed that both the numerical equation and the finite element simulations are able to capture the deformation of the finger under the incrementally increased internal pressure.

The actual bending deformations occurring at respective pressures of 0–0.7 MPa are depicted in Fig. 6 for both the experimental and FEA results. A direct comparison between experimental and FEA results shows that the bending deformations are qualitatively similar under the same cavity pressure. In particular, in the FEA and experimental analysis, a steeper rise in bending is observed up until the applied pressure of 0.5 MPa; the changes occurring between the 0.5 MPa and 0.7 MPa are relatively small. For example, at the end of 0.1 MPa, the downward displacement (measured at the tip of a single finger) was approximately 5 mm in the FE simulation. At that same state, the experimental result showed a displacement of 5.3 mm. Similar to the observations made for the bending angle, it is clear that the sensitivity of the displacements to pressures up to 0.3 MPa are more noticeable than those observed at pressures between 0.4 MPa and 0.7 MPa. For example, only about an 8% increase in displacement occurred between the cases with loads of 0.6 MPa and 0.7 MPa. This suggests that for the contact-free case, a further increase in cavity pressure might not improve the performance of the actuator.

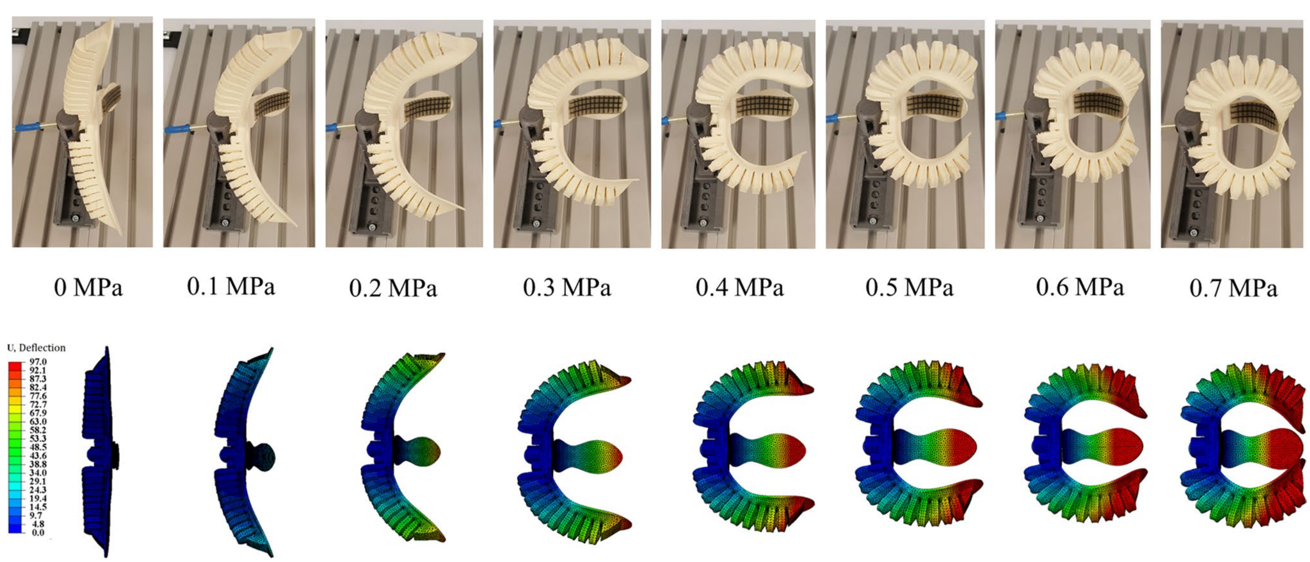

Fig. 6 The experimental and FEA results covering the bending deformation of the soft robotic gripper for the cavity pressures of 0 to 0.7 MPa

4.2 Grasping Experiments and Simulation

Potential differences from the sensor were measured and calibrated using gripping force with cavity pressure. The grasping response of the soft robotic gripper was examined under cavity pressures ranging from 0 to 0.7 MPa. The air leakage test of the gripper was conducted in a water tank. The visual test was accomplished by applying the pressurized air in the cavities of the soft gripper. No leakage was observed up to 0.8 MPa. The results show that power grasping starts after the pressure reaches 0.3 MPa (Fig. 8). To apply a higher force on the targeted spherical object, the air pressure was increased to 0.7 MPa. The gripping force on the spherical object was also measured using a manipulandum with a static load cell in the 10 N measurement range. The cavity pressure versus gripping force for the soft robotic gripper are also shown in Fig. 7. When the cavity pressure was stabilized to 0.4 MPa, the gripping force was measured as 2.85 N. It can also be noticed that the variation of the contact force with the applied cavity pressure is almost linear. Insets in Fig. 7 show the typical grasping state in the experiment and the FE model at an applied cavity pressure of 0.47 MPa, which corresponds to a maximum effective von Mises stress of 6.765 MPa around the different compartments of the gripper. At this point, the contact force measured from the finite element simulation was about 3.75 N; it increased to an approximate value of 8.0 N at 0.7 MPa of pressure. The contact forces predicted by the model were slightly different from those measured in the experiment, especially for the relatively low and relatively

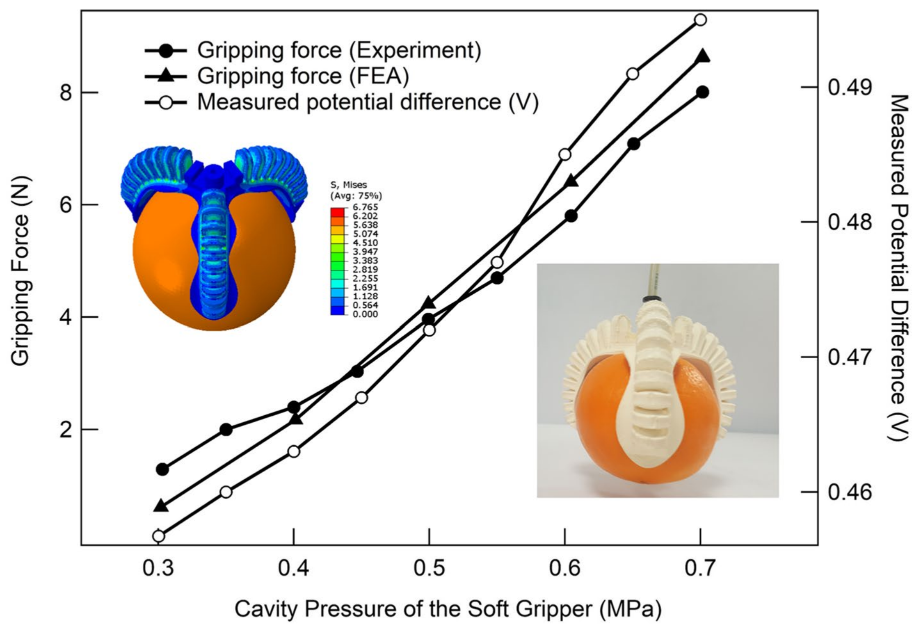

Fig. 7 The cavity pressures versus gripping force for the soft robotic gripper

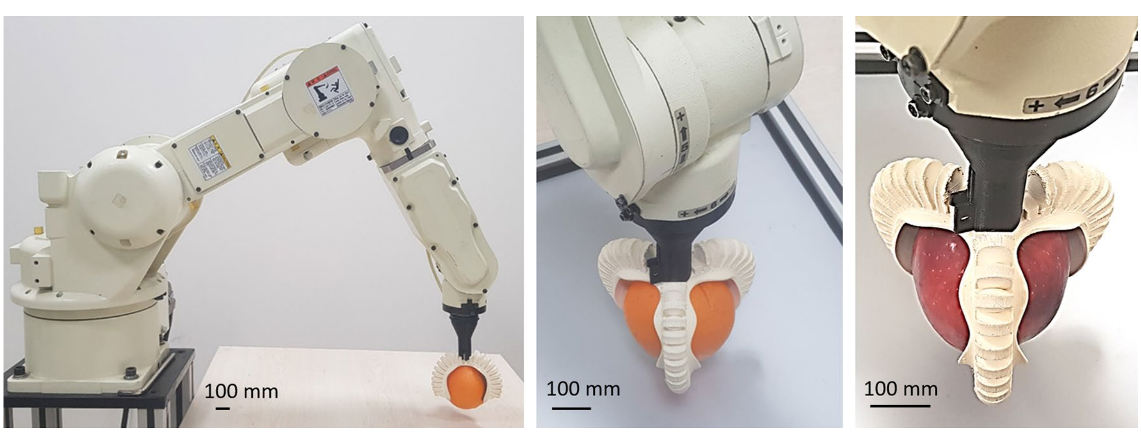

Fig. 8 The demonstration of the power grasp capability of the prototype soft gripper installed on an industrial robot using an orange (*left, center*) and an apple (*right*)

high pressures. However, the observed contact forces for the experiment and the finite element analyses were very close at pressures of 0.4 MPa and 0.6 MPa. The discrepancies between the experiment and the model at the extreme magnitudes of internal pressure may result from differences in the contact relations used in the finite element modeling and the actual experiment. Notwithstanding, a reasonable coherence was observed between the experimental results and model counterparts in the various test cases (Fig. 7). The gripping force of the fingers was measured using an experimental setup shown in Fig. 4. Upon applying the pressurized air, the fingers apply the gripping force on the object while bending. The load-cell is used to measure the applied gripping force.

5 Discussion

The results obtained from both the experiment and the finite element simulations showed that the pneumatically driven soft gripper is able to power grasp spherical objects with diameters ranging from 54 to 120 mm. A comparison was made between the experimental results and the model counterparts to verify the measured gripping forces that were exerted at different magnitudes of pressure. The manufactured soft gripper was able to produce the required amount of bending force to power grasp objects without causing any damage up to cavity pressures of 0.7 MPa.

In addition, the numerical analysis was used to confirm the experimental and FEA results. After enabling the grasping capability, the power grasping quality of the monoblock three-finger soft robotic gripper was determined by using the measured gripping force and bending angle versus cavity pressure parameters. The ratio of the maximum cavity pressure (input pressure) to the maximum gripping force in this study was compared with the ratio calculated for a silicon-based soft gripper from a study by Wu et al. [30]. The overall ratios that were calculated based on the experimental results are 0.015 MPa/N for the TPU-based gripper and 0.0875 MPa/N for the silicon-based gripper. It should be noted that the resolution range of the TPU-based gripper is 5.8 times greater than the resolution range of the silicon-based gripper.

The embedded soft force sensor design is suitable for receiving force feedback, as it produced a reliable response over a wide range of applied force. The maximum gripping force obtained from the FE model (8.0 N) was similar to that recorded in the experiment (7.8 N). The slight difference between these two values can be attributed to the difficulty in modeling the exact frictional contact details used in the experiment.

Recent experimental studies completed by the authors [20, 31, 32] demonstrate that incorporating IL into a photopolymer creates a pressure-sensitive layer that increases the controllability on the soft force sensor performance. The use of this additively manufactured soft force sensor between the gripper and the grasped object was found to increase the functionality of the three-finger soft robotic gripper, as the experimental results revealed that the soft force sensor can provide the feedback needed to achieve an accurate power grasp.

The radius of curvature of the finger must be carefully designed to achieve power grasping of spherically shaped objects. Each finger should be designed with a defined radius of curvature via analytical formulation so that it will apply a nearly equal amount of force to successfully grasp the object; if the forces applied by each finger are not equal, the grasped object may slip. The incorporation of the soft force sensor into the design can provide the data needed to ensure that equal forces are applied in real-time for the specified radius of curvature.

As reorientation of the gripper or re-grasp of an object is required for successful power grasping, sensors are used to provide the feedback needed to adjust the power grasping quality of the gripper. Increasing the number of taxels in the sensor allows us to measure the contact force at additional locations along the finger, providing us with augmented power grasping at the associated contact points. It is noted that different sensor configurations can be fabricated by using various types of taxel structures for the design of the sensor. In addition, the embedded soft force sensors can be placed at distinct points along the soft finger to collect force measurements at specific contact regions when grasping an object. Moreover, the design and additive manufacturing process for the soft force sensor can be varied in terms of geometry and material composition, depending on the required application. In particular, the parameters for the sensor used in this study (such as IL concentration, IL layer thickness, and degree of polymerization) can be modified to produce a sensor with higher sensitivity. The monoblock three-finger gripper can be installed on an industrial robot using only a flange (as shown in Fig. 8), and the resulting system has a low number of component parts.

6 Conclusions

In the current work, a custom-designed monoblock soft robotic gripper with three fingers and an embedded soft force sensor was produced by additive manufacturing and was installed on an industrial robot arm. Experimental, numerical and finite element analyses were conducted for evaluating the power grasping performance of the custom gripper under contact-free conditions as well as in grasping load scenarios with pressures that are typically used in industry. The experimental, analytical and FEA results indicate that the soft force sensors integrated into the robotic gripper enable the power grasping of spherical objects having diameters that range between 54 and 120 mm. The embedded soft force sensors on each finger of the gripper were found to be capable of adequately measuring the gripping force to ensure an accurate power grasp, and the calibrated multi-material soft force sensor designed to receive the force feedback is capable of being used for controlling the power grasping when the soft robotic fingers are grasping a spherical object. This study contributes the validation of the use of additive manufacturing to produce novel soft robotic equipment for applications in the agriculture and biomedical sectors as well as in the automobile industry. In the future, additive manufacturing of all components including sensors and grippers will be investigated, in which sensors will be directly printed on the robotic gripper.

Supplementary Information The online version contains supplementary material available at (https://doi.org/10.1007/s12541-021-00479-0)

Acknowledgements The authors wish to thank Mr. T. Gulnergiz for building the data acquisition system for the fabricated soft force sensor and to Mr. C. Candas for assisting in the technical drawing.

References

1. Trivedi, D., Rahn, C. D., Kier, W. M., & Walker, I. D. (2008). Soft robotics: Biological inspiration, state of the art, and future research. *Applied Bionics and Biomechanics, 5,* 99–117.
2. Albu-Schäffer, A., Eiberger, O., Grebenstein, M., Haddadin, S., Ott, C., Wimbock, T., et al. (2008). Soft robotics: From torque feedback controlled lightweight robots to intrinsically compliant systems. *IEEE Robotics & Automation Magazine, 15,* 20–30.
3. Amend, J. R., Brown, E. M., Rodenberg, N., Jaeger, H. M., & Lipson, H. (2012). A positive pressure universal gripper based on the jamming of granular material. *IEEE Trans Robot., 28,* 341–350.
4. Hu, W., & Alici, G. (2020). Bioinspired three-dimensional-printed helical soft pneumatic actuators and their characterization. *Soft Robotics, 7*(3), 267–282.
5. Sun, T., Chen, Y., Han, T., Jiao, C., Lian, B., & Song, Y. (2020). A soft gripper with variable stiffness inspired by pangolin scales, toothed pneumatic actuator and autonomous controller. *Robot CIM-INT Manufacture, 61,* 1–12.
6. Zolfagharian, A., Kouzani, A. Z., Khoo, S. Y., Moghadam, A. A. A., Gibson, I., & Kaynak, A. (2016). Evolution of 3D printed soft actuators. *Sensors and Actuators A: Physical, 250,* 258–272.
7. Yang, H., Lim, J. C., Liu, Y., Qi, X., Yap, Y. L., Dikshit, V., et al. (2017). Performance evaluation of projet multi-material jetting 3D printer. *Virtual and physical prototyping, 12,* 95–103.
8. Wang, Z., & Hirai, S. (2016, December). A 3D printed soft gripper integrated with curvature sensor for studying soft grasping. In *2016 IEEE/SICE International Symposium on System Integration (SII)* (pp. 629-633). IEEE..
9. Mazzolai, B., Margheri, L., Cianchetti, M., Dario, P., & Laschi, C. (2012). Soft-robotic arm inspired by the octopus: II. From artificial requirements to innovative technological solutions. *Bioinspiration Biomimetics, 7,* 1–14.
10. Margheri, L., Laschi, C., & Mazzolai, B. (2012). Soft robotic arm inspired by the octopus: I. From biological functions to artificial requirements. *Bioinspiration. Biomimetics., 7,* 1–12.
11. Drotman, D., Ishida, M., Jadhav, S., & Tolley, M. T. (2019). Application-driven design of soft 3-D printed, pneumatic actuators with bellows. *IEEE/ASME Transaction on Mechatronics., 24,* 78–87.
12. Ku, S., Myeong, J., Kim, H., & Park, Y. (2020). Delicate fabric handling using A soft robotic gripper with embedded microneedles. *IEEE Robotics and Automation Letter., 5,* 4852–4858.
13. Champatiray, C., Mahanta, G. B., Pattanayak, S. K., & Mahapatra, R. N. (2020). Analysis for material selection of robot soft finger used for power grasping. In B. Deepak, D. Parhi, & P. Jena (Eds.), *Innovative Product Design and Intelligent Manufacturing Systems*. Springer, Newyork: Lecture Notes in Mechanical Engineering.
14. Alici, G. (2009). An effective modelling approach to estimate nonlinear bending behaviour of cantilever type conducting polymer actuators. *Sensors and Actuators B Chemical, 141*(1), 284–292.
15. Miron, G., Bédard, B., & Plante, J. S. (2018). Sleeved bending actuators for soft grippers: A durable solution for high force-to-weight applications. *Actuators, 7*(3), 1–16.
16. Thuruthel, T.G., Haider Abidi, S., Cianchetti, M., Laschi, C., Falotico, E. (2019). A bistable soft gripper with mechanically embedded sensing and actuation for fast closed-loop grasping arXiv:1902.04896 [cs.RO]
17. Lu, N., & Kim, D. H. (2013). Flexible and stretchable electronics paving the way for soft robotics. *Soft Robotics, 1,* 53–62.
18. Yildiz, S. K., Mutlu, R., & Alici, G. (2016). Fabrication and characterization of highly stretchable elastomeric strain sensors for prosthetic hand applications. *Sensors Actuators A: Physical, 247,* 514–521.
19. Amjadi, M., Kyung, K.-U., Park, I., & Sitti, M. (2016). Stretchable, skin-mountable, and wearable strain sensors and their potential applications: A review. *Advanced Functional Material, 26,* 1678–1698.
20. Emon, M. O. F., Lee, J., Choi, U. H., Kim, D., Lee, K., & Choi, J. (2019). Characterization of a soft pressure sensor on the basis of ionic liquid concentration and thickness of the piezoresistive layer. *IEEE Sensor J, 19,* 6076–6084.
21. Ohno, H. (2007). Design of ion conductive polymers based on ionic liquids. *Macromolecular Symposia, 249,* 551–556.
22. Dilibal, S., Sahin, H., & Celik, Y. (2018). Experimental and numerical analysis on the bending response of the geometrically gradient soft robotics actuator. *Archives of Mechanics., 70,* 1–13.
23. Christa, J. F., Aliheidaria, N., Amelia, A., & Potschke, P. (2017). 3D printed highly elastic strain sensors of multiwalled carbon nanotube/thermoplastic polyurethane nanocomposites. *Materials and Design, 131,* 394–401.
24. Elango, N., & Marappan, R. (2011). Analysis on the fundamental deformation effect of a robot soft finger and its contact width during power grasping. *The International Journal of Advanced Manufacturing Technology, 52,* 797–804.
25. Raja, K. V., & Malayalamurthi, R. (2011). Assessment on assorted hyper-elastic material models applied for large deformation soft finger contact problems. *International Journal of Mechanics and Material Design, 7,* 1–7.
26. Ogden, R. W., Saccomandi, G., & Sgura, I. (2004). Fitting hyperelastic models to experimental data. *Computational Mechanics, 34,* 484–502.
27. Sasso, M., Palmieri, G., Chiappini, G., & Amodio, D. (2008). Characterization of hyperelastic rubber-like materials by biaxial and uniaxial stretching tests based on optical methods. *Polymer Testing, 27,* 995–1004.
28. Systèmes, D. (2013). *Abaqus Analysis User's Manual*. Providence, USA: Dassault Systèmes.
29. Ciocarlie, M., Miller, A., Allen, P. (2005). Grasp analysis using deformable fingers, In: IEEE/RSJ International Conference on Intelligent Robots and Systems, Edmonton, Canada 4122–4128.

30. Wu, Z., Li, X., & Guo, Z. (2019). A novel pneumatic soft gripper with a jointed endoskeleton structure. *Chinese Journal of Mechanical Engineering, 32*(1), 1–12.
31. Lee, J., Emon, M. O. F., Vatani, M., & Choi, J. W. (2017). Effect of degree of crosslinking and polymerization of 3D printable polymer/ionic liquid composites on performance of stretchable piezoresistive sensors. *Smart Materials and Structures, 26*(3), 035043.
32. Emon, M. O. F., Alkadi, F., Philip, D. G., Kim, D., Lee, K., & Choi, J. (2019). Multi-Material 3D printing of a soft pressure sensor. *Additive Manufacturing, 28,* 629–638.
33. Abayazid, F. F., & Ghajari, M. (2020). Material characterisation of additively manufactured elastomers at different strain rates and build orientations. *Additive Manufacturing, 33,* 101160.
34. Hohimer, C., Christ, J., Aliheidari, N., Mo, C., & Ameli, A. (2017, April). 3D printed thermoplastic polyurethane with isotropic material properties. In *Behavior and Mechanics of Multifunctional Materials and Composites 2017* (Vol. 10165, p. 1016511). International Society for Optics and Photonics

Savas Dilibal is an Associate Professor in the Department of Mechatronics Engineering at the Istanbul Gedik University, Turkey. He received BS in System Engineering from Army Academy, M.Sc. in Mechanical Engineering from Istanbul Technical University, and Ph.D. in Materials Engineering from Yildiz Technical University. He completed a postdoctoral fellowship at the University of Illinois at Urbana-Champaign. He was an adjunct faculty in the Mechanical Engineering Department at the University of Akron. He worked in a NASA-funded, SMA-related project. He is currently the head of Mechatronics Engineering Department at Istanbul Gedik University. He is also the director of the Robot Technology Research, Application Center.

Haydar Sahin is currently an Assistant Professor in the Department of Mechatronics Engineering, Istanbul Gedik University, Turkey. He received BS in Mechanical Engineering from Istanbul Technical University. Additionally, he received his M.Sc. in vehicle kinematics modeling and control from the Department of Mechanical Engineering, Rochester Institute of Technology, USA, and his Ph.D. degree in multibody dynamics modeling of the railway vehicles from Department of the Mechanical Engineering, Marmara University, Turkey, in 1997 and 2014, respectively. His research interests include multibody dynamics design of robotics, modular robotics, symbolic mathematics, mechatronics system design, and vehicle system dynamics.

Josiah Owusu Danquah is an assistant professor in the department of Civil and Environmental Engineering at Cleveland state University (CSU). He received his undergraduate training from the University of Science and Technology (KNUST) in Ghana and his Ph.D. from the University of Akron, Ohio. Dr. Owusu-Danquah's research focuses on smart materials, computational mechanics, finite element simulation and the optimization of engineering structures. He currently serves as the director of the Structures and Foundation Graduate Program in the Civil and Environmental Engineering Department. He is a member of the American Society of Civil Engineers (ASCE) and American Society for Engineering Education (ASEE).

Md Omar Faruk Emon is a Teaching Support Specialist III in the Meinig School of Biomedical Engineering at Cornell University. He received the B.S. degree in Mechanical Engineering in 2012 from Bangladesh University of Engineering and Technology, Dhaka, Bangladesh, and PhD degree in Mechanical Engineering in 2020 from the Department of Mechanical Engineering at the University of Akron, Ohio, USA. His research interest lies in the field of 3D-printing of stretchable electronics.

Jae-Won Choi is an Associate Professor in the Department of Mechanical Engineering at the University of Akron. He received B.S., M.S. and Ph.D. degrees from Pusan National University, S. Korea in 1999, 2001, and 2007, respectively. His research interests include additive manufacturing of smart structures; and multi-scale, multimaterial additive manufacturing. He serves as an associate editor in Additive Manufacturing; editorial board member in International Journal of Precision Engineering and Manufacturing (also Green Technology); editor in The Korean Society of Manufacturing Process Engineers. He is a member of ASME, SME, and SPIE.